

Withdrawal Strength of Pneumatically Driven Steel Pin Connections in Cold-Formed Steel Light-Frame Construction

R. Serrette, A.M.ASCE¹; D. Nolan²; and B. Kifle³

Abstract: Pneumatically driven steel pins have been successfully used for attaching structural sheathing to cold-formed steel framing in both load-bearing and nonload-bearing applications. The design of these types of connections is exclusively based on published manufacturer data. Attempts to analytically quantify/estimate the shear and withdrawal (tensile) strength of pin connections is nearly nonexistent. This paper proposes a mechanics-based equilibrium model for withdrawal strength and presents test data for wood structural panels connected to cold-formed steel with pneumatically driven steel pins. The tests include a range of wood panel and cold-formed steel thicknesses commonly found in light-frame construction. Using the proposed model, empirically modified to reflect observed behavior, equations are presented to estimate the withdrawal strength of connections made with helically knurled pins. The proposed equations are shown to provide reasonably good estimates of strength with a reliability consistent with that of the more commonly used screw fastener. DOI: 10.1061/(ASCE)ST.1943-541X.0001916. © 2017 American Society of Civil Engineers.

Author keywords: Cold-formed steel; Withdrawal/tension connection; Pneumatic driven pins; Wood structural panels; Light-frame construction; Metal and composite structures.

Introduction

In load-bearing and nonload-bearing light-frame construction, structural panels are typically attached to cold-formed steel (CFS) members with either screws or hardened steel pins. Morgan et al. (2002) also studied the use of specially purposed adhesives in combination with these mechanical fasteners and applications with steel staples. Steel pins are manufactured with either a smooth or deformed shank, and they are capable of providing relatively high connection strength with reliable performance. Yet, despite a history of successful use, scant attention has been directed toward the development of basic analytical expressions to estimate shear and withdrawal/tensile connection strength in light-frame CFS construction. An oft-cited concern regarding the development of such expressions is the proprietary nature of the pin shank. This concern is, however, also applicable to screws in which thread shape, spacing, and depth can be different between screws with the same basic callout.

Steel pins used in CFS light-frame construction are manufactured from hardened steel and finished with a sharp ballistic point and flat or bugle head—flat head being more common. The pin-head diameter is typically two to three times the pin-shank outside diameter, and the pin shank may be smooth or knurled. Knurling is

primarily used to increase the holding resistance of the pin in steel framing by (1) increasing contact area; (2) allowing for a coarser/rougher contact surface; and (3) depending on the helix angle, bearing on the knurled tooth surface during withdrawal. Fig. 1 illustrates basic knurl patterns and defines common terms associated with these patterns.

As described by Nolan (2009), the action of inserting a steel pin through the thickness of a structural panel, piercing of the steel framing by pin's ballistic point, and subsequent in-plane radial deformation of the steel around the pin shank provides the basic mechanism for holding the pin. Conceptually, the action by which a pin is inserted and holds in CFS framing is akin to inserting an ice pick into a block of rubber. The magnitude of the clamping force created at the pin–CFS framing contact surface effectively controls the connection performance.

Where structural components are subjected to net outward pressures—wall and roof sheathing (Fig. 2)—reliable quantification of the withdrawal/tensile strength of pin connections is critical. Under withdrawal loads, limit states in the CFS framing, sheathing, and the connection need to be addressed. Framing and sheathing limit states are currently addressed in the American Iron and Steel Institute's (AISI) cold-formed steel specification [AISI S100 (AISI 2012)], and sheathing material by manufacturers, in the case of wood structural panels (WSP), the American Wood Council Design Specification [AWC NDS (AWC 2014)]. For the withdrawal connection, three basic limit states require consideration: (1) pin pull-out (PO) from the framing; (2) pin-head bearing in the sheathing, leading ultimately to pull through (PT) the sheathing; and (3) pin fracture in tension. Like screw fasteners, pin tensile (fracture) strength is addressed by the pin manufacturer—generally, the material strength of steel pins is four to eight times that of the common 228- to 345-MPa yield steels used in light-frame construction in the United States.

Fig. 3(a) illustrates the limit states of PO and PT for wood structural panel sheathing attached to CFS, and Fig. 3(b) shows the equilibrium model proposed in this paper to address these limit states.

¹Professor, Dept. of Civil Engineering, Santa Clara Univ., 500 El Camino Real, Santa Clara, CA 95053 (corresponding author). E-mail: rserrette@scu.edu

²General Manager, ET&F Fastening Systems, Inc., 29019 Solon Rd., Solon, OH 44139. E-mail: dnolan@etf-fastening.com

³Manager, California Expanded Metal Company Engineering Laboratory, 1001-A Pittsburg-Antioch Hwy., Pittsburg, CA 94565. E-mail: bkifle@cemcosteel.com

Note. This manuscript was submitted on September 22, 2016; approved on June 15, 2017; published online on October 23, 2017. Discussion period open until March 23, 2018; separate discussions must be submitted for individual papers. This paper is part of the *Journal of Structural Engineering*, © ASCE, ISSN 0733-9445.

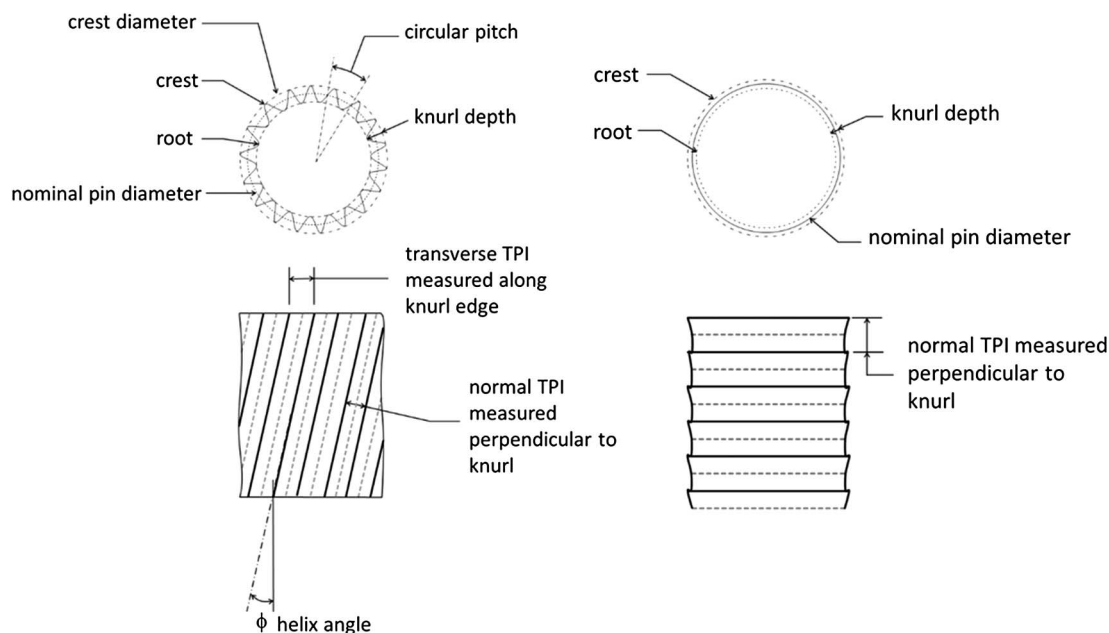


Fig. 1. Steel pins

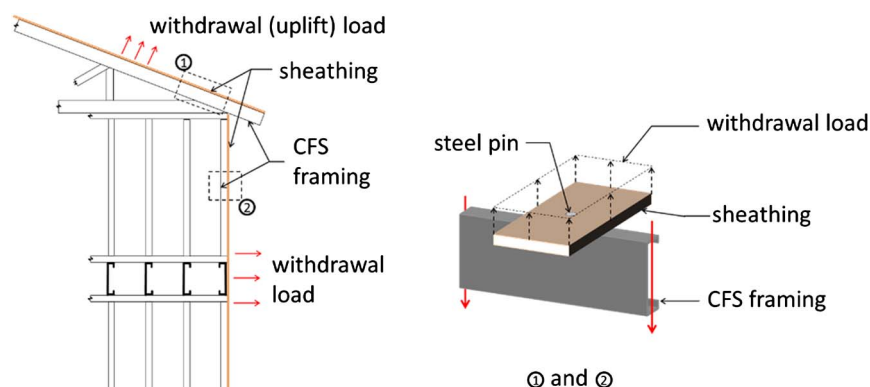


Fig. 2. Withdrawal/tension loading

As shown in Fig. 3(b), the pin is held in the CFS by a friction force P_{f-CFS} that provides the pin nominal PO resistance P_{npo} . Pull-through strength P_{npt} is provided by a combination of bearing under the pin head (P_{brmg}) and friction along the pin shank (P_{f-WSP}). Using the proposed model, the nominal withdrawal strength P_n may be estimated by using Eq. (1). P_{npo} in Eq. (1) is a function of an effective pin-CFS friction coefficient (μ_{f-CFS}), the pin shank (d), and the thickness (t) and the tensile strength (F_u) of the CFS framing. P_{npt} is a function of an effective pin-WSP friction coefficient (μ_{f-WSP}), d , diameter of the pin head (d_{hd}), thickness of the WSP (t_{WSP}), and the bearing stiffness (k_{brmg}) in the WSP

$$P_n = \min \left[\begin{array}{l} P_{npo} = P_{f-CFS} = g_1(\mu_{f-CFS}, F_u, d, t) \\ P_{npt} = P_{f-WSP} + P_{brmg} = g_2(\mu_{f-WSP}, d, d_{hd}, t_{WSP}, k_{brmg}) \end{array} \right] \quad (1)$$

Based on a series of pullout tests, Serrette and Nolan (2015) suggested that μ_{f-CFS} may range between 0.42 and 0.60. Their

recommendation was based on test results for a single WSP thickness and CFS framing thicknesses between 0.84 and 1.73 mm (33 and 68 mil). The *Wood handbook* (FPL 2010) notes that for wood, the magnitude of the friction coefficient is a function of the moisture content and roughness of the wood and “characteristics of the opposing surface.” The handbook suggests that the kinetic friction coefficient for smooth wood against a hard smooth surface may range between 0.3 and 0.5 when the wood is dry, between 0.5 and 0.7 at intermediate moisture contents, and may be as high as 0.9 near the fiber saturation point. On the basis of “extensive testing . . . in accordance with [ASTM D1761 (ASTM 2012)],” APA—The Engineered Wood Association (2012) recommended that the unadjusted allowable withdrawal strength of nails in WSP be related to the “equivalent specific gravity” of the WSP by Eq. (2)

$$p = 9.52 G_{equiv}^{5/2} dL \quad (2)$$

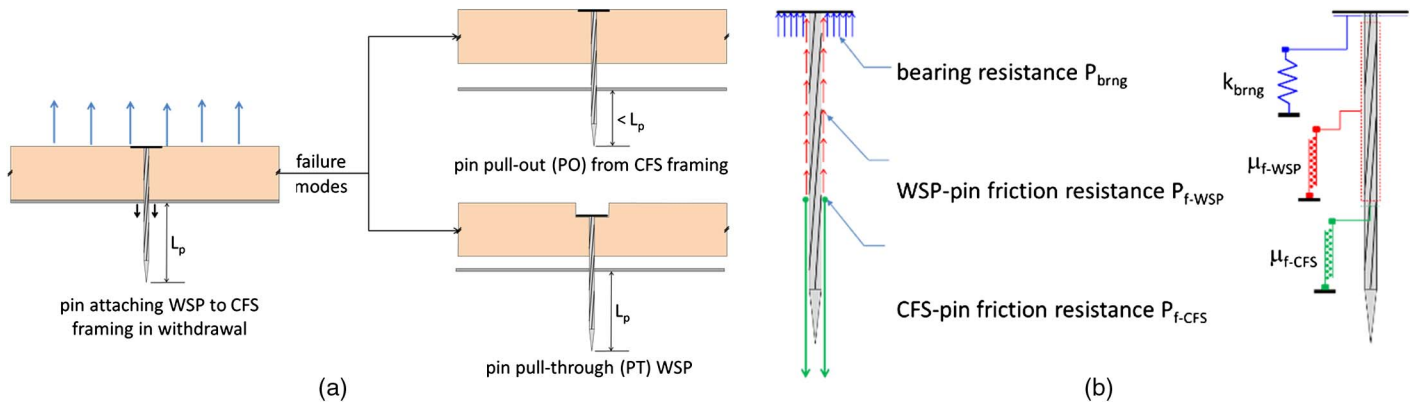


Fig. 3. (a) PO and PT limit states; (b) pin equilibrium model

where d = nail shank diameter; L = depth of penetration in the WSP; G_{equiv} = equivalent specific gravity; and 9.52 coefficient = essentially a friction pressure (MPa or N/mm²). APA—The Engineered Wood Association defines an equivalent specific gravity G_{equiv} , as opposed to specific gravity G , because WSP is a composite material compared with a single-species wood member. Recommended values of G_{equiv} for dry service conditions for both plywood (PWD) and oriented strand board (OSB) ranged between 0.40 for smooth-shank nails and 0.70 for ring-shank (annularly threaded) nails.

The *Wood handbook* (FPL 2010) gives the maximum (peak) withdrawal strength of bright common (smooth) nails by Eq. (3); d and L are as defined in Eq. (2), and G is the specific gravity of the wood member. Eqs. (2) and (3) suggest that as the density of wood or WSP increases, fastener withdrawal strength will also increase. Thus, for the pull-through limit state, as the WSP around the nail head is compressed, the density of the WSP in the region of the pin head is increased, and this change in density should translate into an increase in pull-through strength

$$p = 54.12G^{5/2}dL \quad (3)$$

Compression of the WSP material at the pin head will also increase the bearing strength at the pin head. APA—The Engineered Wood Association (2013) reported results from a large sample of bearing tests on 9.52-, 15.1-, and 18.3-mm WSP materials at 0.508 and 1.02 mm of bearing deformation. The APA—The Engineered Wood Association report showed that (1) bearing strength increased with bearing deformation; (2) bearing strength increase was not directly proportional to bearing deformation; and (3) thicker WSP had a lower bearing strength. The average specific gravity of the panels (OSB and PWD) ranged between 0.56 and 0.60, with a 25th percentile range between 0.53 and 0.56. The coefficient of variation for the bearing values ranged between 24.0 and 30.6%. Thus, with increased pull-through deformation, exceeding 1.02 mm, it is expected that WSP bearing strength will increase until the pin head begins to break out the nonbearing face of the WSP.

On the basis of the preceding discussion, Eq. (1) may be rewritten as shown in Eq. (4). Eq. (4) is formatted to facilitate comparisons of connection withdrawal strength for pin fasteners with alternative shank configurations and head styles

$$P_n = \min \left[\begin{array}{l} P_{\text{npo}} = \xi dt F_u \\ P_{\text{npt}} = A_{\text{brng}} F_{\text{brng}} + \beta G^{5/2} \pi d L_{\text{WSP}} \end{array} \right] \quad (4)$$

where $\xi = \mu_{f-\text{CFS}}$; A_{brng} = net bearing area under the pin head; F_{brng} = bearing force under the pin head at a defined level of

bearing deformation; β = friction stress between the pin shank and WSP; and L_{WSP} = thickness of the WSP not compressed by the pin head.

Experimental Program

Scope

A review of International Code Council-Evaluation Services (ICC-ES) reports from a representative group of U.S. pin manufacturers [ESR 3059 (ICC-ES 2014), ESR 2962 (ICC-ES 2015a), ESR 2961 (ICC-ES 2015b), ESR 3380 (ICC-ES 2015c), ESR 2174 (ICC-ES 2016a), ESR 5380 (ICC-ES 2016b), and ESR 1641 (ICC-ES 2016c)] reveal that for CFS light-frame construction (including curtain walls), pin-shank diameters generally range between 2.54 and 3.81 mm, with pin-head diameters between 6.35 and 8.26 mm. Knurl patterns were primarily helical and horizontal, with the helix pattern being the most common. On the basis of this information, a broad series of withdrawal tests were conducted with helically knurled pins to explore the ξ , F_{brng} , β , and L_{WSP} parameters in Eq. (4).

The experimental program included two nominal pin diameters, 2.54 and 3.66 mm, with 6.35- and 7.94-mm head diameters, respectively. The pin heads were flat, and the shank was helically knurled with 1.26 threads/mm (measured perpendicular to the thread). The pins and tooling for installation of the pins were sourced from ET&F Fastening Systems (Solon, Ohio); the pins were independently (independent of the project team and pin manufacturer) and randomly sampled. The CFS framing thickness ranged from 0.84 to 3.00 mm (33 to 118 mil), with minimum specified yield strengths between 228 and 345 MPa. Wood structural panels included Structural I OSB, OSB rated sheathing (called OSB in this paper), and Structural I PWD; all materials were sourced from local lumber and hardware stores. The scope of the test program is summarized in Table 1. For each connection configuration noted in Table 1, six identical tests were performed for a total of 162 tests. The number of repeat tests was based on the recommendations AISI S100, Chapter F, Section F1.

Material and Geometric Properties, and Ambient Test Conditions

Material and geometric properties of the CFS framing used in the test program are summarized in Table 2. Tensile coupons [ASTM A370 (ASTM 2016)] were taken from the CFS framing test components, parallel to framing length. Except for the 0.84- and

Table 1. Scope of Experimental Program

Pin diameter, d (mm)	Head diameter, d_{hd} (mm)	Sheathing thickness and grade	Designated framing thickness [mm (mils)]	Measured framing thickness, t_m (mm)	Measured framing yield strength, F_{ym} (MPa)	Measured framing tensile strength, F_{um} (MPa)
2.54	6.35	11.1-mm OSB rated sheathing	0.84 (33)	0.88	311	374
			1.37 (54)	1.41	400	455
			2.46 (97)	2.55	284	353
		11.9-mm OSB rated sheathing	0.84 (33)	0.88	311	374
			1.37 (54)	1.41	400	455
			2.46 (97)	2.55	284	353
		15.1-mm OSB rated sheathing	0.84 (33)	0.88	311	374
			1.37 (54)	1.41	400	455
			2.46 (97)	2.55	284	353
		18.3-mm OSB rated sheathing	0.84 (33)	0.88	311	374
			1.37 (54)	1.41	400	455
			2.46 (97)	2.55	284	353
3.66	7.92	15.1-mm OSB rated sheathing	1.73 (68)	1.78	411	492
			2.46 (97)	2.55	284	353
			3.00 (118)	3.33	289	362
		18.3-mm OSB rated sheathing	1.73 (68)	1.78	411	492
			2.46 (97)	2.55	284	353
			3.00 (118)	3.33	289	362
		18.3-mm Structural I OSB	1.73 (68)	1.78	411	492
			2.46 (97)	2.55	284	353
			3.00 (118)	3.33	289	362
		28.6-mm OSB rated sheathing/Sturd-I-Floor	1.73 (68)	1.78	411	492
			2.46 (97)	2.55	284	353
			3.00 (118)	3.33	289	362
		28.6-mm Structural I PWD	1.73 (68)	1.78	411	492
			2.46 (97)	2.55	284	353
			3.00 (118)	3.33	289	362

3.00-mm (33- and 118-mil) framing, the ratios of measured to minimum design thickness (t_m/t_{des}) were between 1.000 and 1.038; a t_m/t_{des} ratio 1.05 is typically considered the threshold above which test design values are required to be reduced. For the 0.84- and 3.00-mm (33- and 118-mil) framing, the t_m/t_{des} ratios were 1.058 and 1.111, respectively. The expected yield and tensile strength ratios (R_y and R_t , respectively) were generally similar to, or less than, the values suggested in AISI's lateral standard [AISI S213 (AISI 2009)].

Wood structural panels for the tests were stored in a dry, sheltered location in the test laboratory. During testing, the relative humidity in the test laboratory varied between 34 and 62%, and the temperature ranged between 15.6 and 32.2°C.

Test Setup

A simple, stiff, concentric loading setup was designed and fabricated for the test program. Each test specimen was configured with the WSP component oriented and connected perpendicular to the CFS framing component (Fig. 4, Stage 1). A specimen was installed in an upper steel fixture with the ends of the WSP component clamped/fixated in the fixture. A lower steel fixture was then installed over the CFS framing (Fig. 4, Stage 2) to create the setup shown in Fig. 4, Stage 3. The lower fixture was attached to a fixed support, and the upper fixture to the movable head of a universal testing machine. The steel fixtures fabricated were 102 mm wide by 12.5 mm thick. The axial stiffness of the vertical legs of the upper and lower fixtures was approximately 2,539 kN/mm, the flexural stiffness of the horizontal plate (conservatively assuming simple supports at its intersection with the vertical legs) was 20 kN/mm, and the flexural stiffness of the 64 mm return plates was 1,012 kN/mm. Thus, the contribution of fixture deformation

to the measured deformation in the WSP-to-CFS framing connection was considered negligible.

The physical WSP-CFS framing contact area was 76.2×88.9 mm, and the unsupported (not clamped by the upper fixture) area of the WSP was 76.2×101.6 mm. The clamped WSP ends, with a 101.6-mm length between clamps, limited flexure of the WSP component. Similarly, the approximately 76.2-mm unsupported length of the CFS framing component limited flexure in this component. Load was applied through the upper fixture, and separation of the WSP and CFS framing was monitored and recorded (Fig. 4, Stage 4). A constant speed, monotonic displacement regime was applied to each specimen. The displacement rate ranged between 2.54 and 3.81 mm/min.

Test Results and Discussion

Connection peak withdrawal strength P_{peak} was primarily governed by either the pin pulling out from the CFS framing or "considerable" bearing deformation in the WSP. Unlike tests that are design to produce failure by a single limit state, the tests reported in this paper reflected actual connection behavior. Where connection behavior was characterized as pin pullout, it was observed to be accompanied by bearing deformation in the WSP component. For the combinations of materials tested, bearing deformation in the WSP was not observed to result in complete pin pull through. Instead, what was observed was considerable bearing deformation in the WSP, typically exceeding 7.62 mm. Thus, in this paper, pull through is defined as a bearing deformation limit state corresponding to 7.62 mm. Figs. 5 and 6 show typical withdrawal responses for the PO and PT limit states—both figures show classic scatter in the response throughout the entire load regime.

Table 2. CFS Framing Properties

ASTM designation	Thickness				Material properties				AISI							
	Designated CFS thickness [mm (mils)]	Minimum CFS thickness, t_{min} (mm)	CFS design, t_{des} (in.)	Measured CFS thickness, t_m (mm)	Minimum specified		Measured		F_y (MPa)	F_u (MPa)	F_{ym} (MPa)	F_{um} (MPa)	$F_{ym}/F_y = R_y$	$F_{um}/F_u = R_t$	R_y	R_t
					F_y	F_u	F_{ym}	F_{um}								
A653M (ASTM 2015) SS Grade 230 or equivalent	0.84 (33)	0.84	0.88	0.88	228	310	311	374	1.058	1.37	1.20	1.5	1.2			
A653M SS Grade 340/1 or equivalent	1.37 (54)	1.37	1.44	1.41	345	448	400	455	1.035	1.16	1.02	1.1	1.1			
A653M SS Grade 340/1 or equivalent	1.73 (68)	1.72	1.81	1.78	345	448	411	492	1.034	1.19	1.10	1.1	1.1			
A653M HSLAS Grade 275 or equivalent	2.46 (97)	2.45	2.58	2.55	276	345	284	353	1.038	1.03	1.02	1.3	1.1			
A653M HSLAS Grade 275 or equivalent	3.00 (118)	3.00	3.15	3.33	276	345	289	362	1.111	1.05	1.05	1.3	1.1			

Note: HSLAS = high strength low-alloy steel; SS = structural steel.

Comparing Figs. 5 and 6, there is one noticeable difference. In the pull-through-type limit state, there appears to be two stages of bearing deformation—an initially soft stage, followed by a stiffening effect. The stiffening effect may be the result of engagement of friction along the pin shank and densification of the WSP in the proximity of the pin head as the pin head compresses the WSP.

Table 3 summarizes the average peak withdrawal strength (P_{peak}) results for each connection configuration tested, along with its coefficient of variation (COV) and the predominant failure mode [either PO or PT]. The COV values varied between 3.5 and 26.0%, with the majority of values (85%) less than 19.0%. Generally, for both pin diameters, Table 3 shows that, for a given WSP thickness, as the CFS framing thickness increased, so did P_{peak} . Similarly, for a given CFS framing thickness, an increase in WSP thickness resulted in an increase in P_{peak} . Thus, the test data suggest that an increase in the thickness of WSP or CFS framing results in an increase in connection strength.

Effects of WSP and CFS Framing Thickness

A closer evaluation of the effects of WSP and CFS framing thickness is shown in Figs. 7 and 8 for the 2.54- and 3.66-mm-diameter pins, respectively. In Fig. 7, the incremental connection strength increase of 0.84- to 1.37-mm (33- to 54-mil) framing is greater than the incremental increase when the thickness is increased from 1.37 to 2.46 mm (54 to 97 mil). This difference may be indicative of a transition in limit state from pullout to pull through as the framing thickness increased for a fixed WSP panel thickness. The argument for a limit-state transition is further supported by the fact that, for the 0.84-mm (33-mil) framing, the difference in connection strength for WSP thicknesses of 11.1–18.3 mm is rather small compared with the differences at 2.46 mm (97 mil). Fig. 7 also shows that there was little difference in the strength of 15.1- and 18.3-mm OSB.

In Fig. 8, where framing thickness varies between 1.73 and 3.00 mm (68 and 118 mil), incremental strength increase caused by framing thickness increase appears to be approximately linear regardless of the WSP thickness. Fig. 8 also shows that there may be no significant strength benefit of Structural I OSB compared with OSB rated sheathing. Also, a comparison of 28.6-mm Structural I PWD with OSB rated sheathing suggests that a maximum strength increase of approximately 12% of Structural I PWD over OSB rated sheathing.

Effect of Pin Size

Larger-diameter pins are typically used in applications with thicker CFS framing. Figs. 9 and 10 compare the strength of the 2.54- and 3.66-mm-diameter pins in connections with 15.1- and 18.3-mm OSB, respectively. Both figures show that higher connection strengths are available with larger pins. Based on the pin equilibrium model presented previously, because larger pins have greater pin-head bearing area and shank friction surface area, higher connection strength is expected.

For CFS framing of 1.37 mm (54 mil) and thicker, Fig. 9 shows a near-parallel proportional strength increase with framing thickness for both pin sizes, with the connection strength of the 3.66-mm-diameter pins being approximately 37% more than that of the 2.54-mm-diameter pins. Fig. 10, on the other hand, shows a steeper strength increase for the larger pin and an approximate doubling in strength for connections with the 3.66-mm-diameter pins compared with the 2.54-mm-diameter pins.

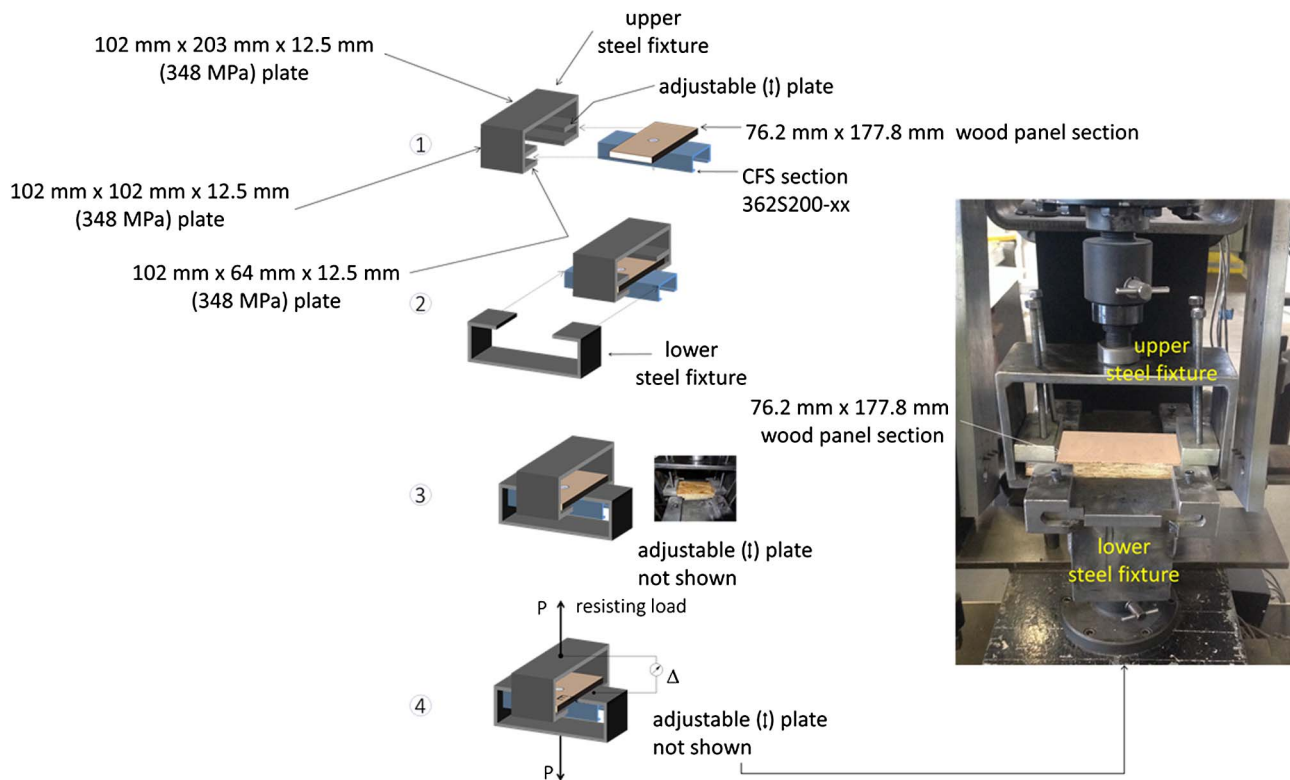


Fig. 4. Test setup (stages of assembly and final setup)

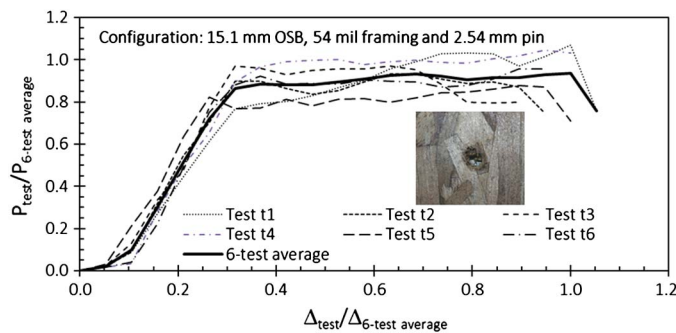


Fig. 5. Typical pull-through-type connection response

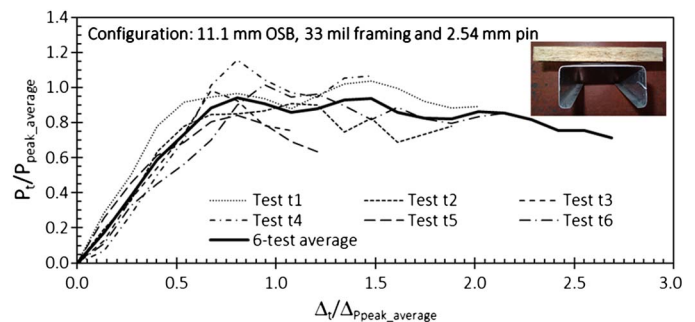


Fig. 6. Typical pullout-type failure mode test result

Design Model

On the basis of the observed behavior and the equilibrium model represented in Eqs. (1) and (4), semiempirical expressions were developed to estimate the withdrawal connection strength of the knurled pins used in the test program.

Nominal Pullout Strength, P_{npo}

As noted previously, penetration of steel pins into CFS framing results in the native steel being deformed radially outward. The result is a tight friction fit between the pin shank and the native steel that ultimately produces pin pullout resistance. The friction provided by the deformed steel is a function of the steel's materials properties. On the basis of the mechanism by which the pin is inserted, and noting that the friction force results from bearing developed from penetration/fracturing of the steel, the tensile strength of the steel is used as the key material property for the pullout strength. Both

hot-rolled and cold-formed steel specifications typically use the tensile strength of steel in bearing strength calculations.

By using the generic expression in Eq. (4), the trends observed in the test data (as presented previously), and regression analysis, Eq. (5) was developed to estimate the connection pullout strength when WSP is attached to CFS framing

$$P_{npo} = 0.36415 \left[e^{(0.0543(\frac{WSP}{d_1}))} \right] \left(\frac{d}{d_1} \right)^{0.30} dtF_u \quad (5)$$

where d = pin diameter (mm); t = CFS framing design thickness (mm); F_u = tensile strength of CFS framing (MPa); d_1 = reference pin diameter = 2.54 mm; and t_{WSP} = nominal thickness of WSP (mm).

Nominal Pull-Through (Bearing) Strength, P_{npt}

By using the generic expression in Eq. (4) for pull through and the trends observed in the test data, Eq. (6) was developed to estimate

Table 3. Average Peak Withdrawal Connection Strength

Pin diameter, d (mm)	Sheathing thickness and grade	Designated framing thickness [mm (mils)]	Measured framing thickness, t_m (mm)	Measured framing yield strength, F_{ym} (MPa)	Measured framing tensile strength, F_{um} (MPa)	Average P_{peak} (N)	Standard deviation of P_{peak} (N)	COV (%)	Predominant failure mode
2.54	11.1-mm OSB rated sheathing	0.84 (33)	0.88	311	374	291	31	10.7	PO
		1.37 (54)	1.41	400	455	645	22	3.5	PO
		2.46 (97)	2.55	284	353	791	78	9.8	PT
	11.9-mm OSB rated sheathing	0.84 (33)	0.88	311	374	382	87	22.7	PO
		1.37 (54)	1.41	400	455	790	205	26.0	PT
		2.46 (97)	2.55	284	353	919	138	15.0	PT
	15.1-mm OSB rated sheathing	0.84 (33)	0.88	311	374	419	88	21.1	PO
		1.37 (54)	1.41	400	455	954	63	6.6	PO
		2.46 (97)	2.55	284	353	1,175	123	10.5	PT
	18.3-mm OSB rated sheathing	0.84 (33)	0.88	311	374	423	40	9.5	PO
		1.37 (54)	1.41	400	455	998	100	10.1	PO
		2.46 (97)	2.55	284	353	1,220	229	18.8	PT
3.66	15.1-mm OSB rated sheathing	1.73 (68)	1.78	411	492	1,507	211	14.0	PO
		2.46 (97)	2.55	284	353	1,612	195	12.1	PT
		3.00 (118)	3.33	289	362	1,905	400	21.0	PT
	18.3-mm OSB rated sheathing	1.73 (68)	1.78	411	492	1,990	294	14.7	PO
		2.46 (97)	2.55	284	353	2,550	371	14.5	PO
		3.00 (118)	3.33	289	362	2,870	323	11.2	PT
	18.3-mm Structural I OSB	1.73 (68)	1.78	411	492	2,017	330	16.4	PO
		2.46 (97)	2.55	284	353	2,634	176	6.7	PO
		3.00 (118)	3.33	289	362	2,877	379	13.2	PT
	28.6-mm OSB rated sheathing/Sturd-I-Floor	1.73 (68)	1.78	411	492	2,290	140	6.1	PO
		2.46 (97)	2.55	284	353	3,101	296	9.5	PO
		3.00 (118)	3.33	289	362	3,477	518	14.9	PT
	28.6-mm Structural I PWD	1.73 (68)	1.78	411	492	2,563	134	5.2	PO
		2.46 (97)	2.55	284	353	3,191	235	7.4	PO
		3.00 (118)	3.33	289	362	3,738	297	8.0	PT

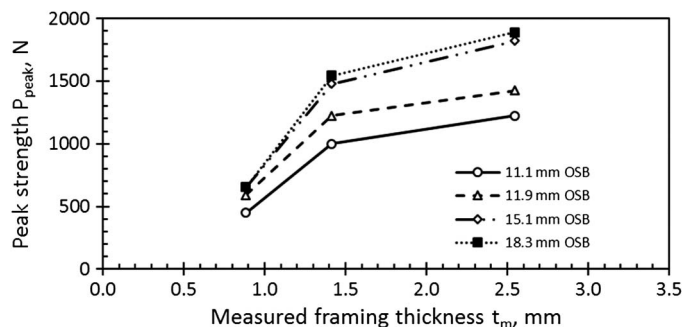
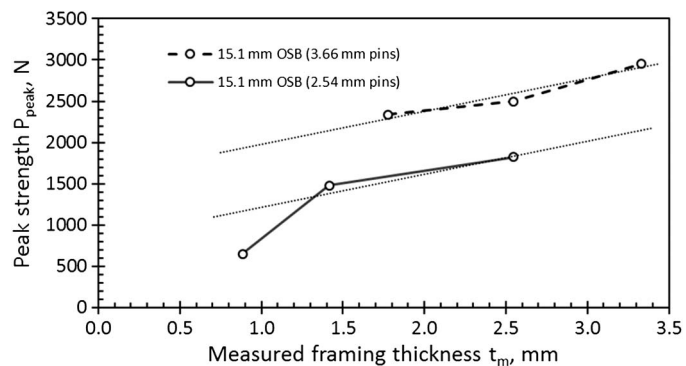
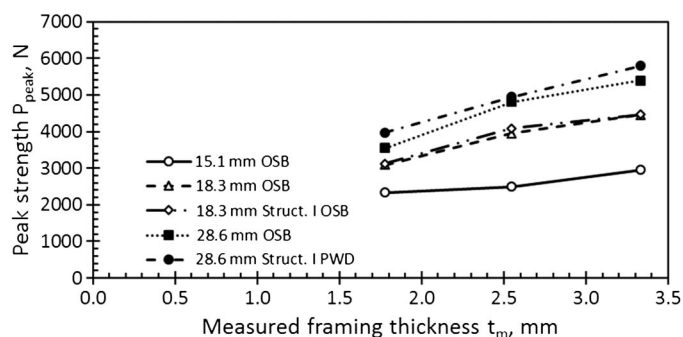
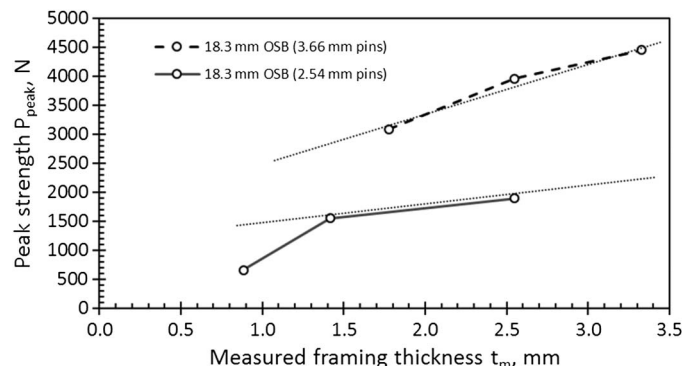
**Fig. 7.** Effects of CFS framing and WSP thickness—2.54-mm-diameter pins**Fig. 9.** Connection peak strength—15.1-mm OSB**Fig. 8.** Effects of CFS framing and WSP thickness—3.66-mm-diameter pins**Fig. 10.** Connection peak strength—18.3-mm OSB

Table 4. Comparison of Measured Peak and Calculated Nominal Withdrawal Strength

Pin diameter, <i>d</i> (mm)	Sheathing thickness and grade	Designated framing thickness	Average	Standard deviation of	COV	Calculated pullout strength,	Calculated pull-through strength,	Calculated connection nominal strength,	<i>P</i> _{peak} / <i>P</i> _{<i>n</i>}
		[mm (mils)]	<i>P</i> _{peak} (N)	<i>P</i> _{peak} (N)	(%)	<i>P</i> _{npo} (N)	<i>P</i> _{npt} (N)	<i>P</i> _{<i>n</i>} (N)	
2.54	11.1-mm OSB rated sheathing	0.84 (33)	291	31	10.7	388	775	388	0.750
		1.37 (54)	645	22	3.5	756	775	756	0.854
		2.46 (97)	791	78	9.8	1,054	775	775	1.021
	11.9-mm OSB rated sheathing	0.84 (33)	382	87	22.7	394	819	394	0.968
		1.37 (54)	790	205	26.0	769	819	769	1.029
		2.46 (97)	919	138	15.0	1,072	819	819	1.123
	15.1-mm OSB rated sheathing	0.84 (33)	419	88	21.1	422	994	422	0.994
		1.37 (54)	954	63	6.6	822	994	822	1.160
		2.46 (97)	1,175	123	10.5	1,147	994	994	1.182
	18.3-mm OSB rated sheathing	0.84 (33)	423	40	9.5	451	1,169	451	0.936
		1.37 (54)	998	100	10.1	880	1,169	880	1.133
		2.46 (97)	1,220	229	18.8	1,228	1,169	1,169	1.043
3.66	15.1-mm OSB rated sheathing	1.73 (68)	1,507	211	14.0	1,793	2,083	1,793	0.841
		2.46 (97)	1,612	195	12.1	1,843	2,083	1,843	0.875
		3.00 (118)	1,905	400	21.0	2,469	2,083	2,083	0.915
	18.3-mm OSB rated sheathing	1.73 (68)	1,990	294	14.7	1,918	2,607	1,918	1.037
		2.46 (97)	2,550	371	14.5	1,973	2,607	1,973	1.293
		3.00 (118)	2,870	323	11.2	2,643	2,607	2,607	1.101
	18.3-mm Structural I OSB	1.73 (68)	2,017	330	16.4	1,918	2,607	1,918	1.051
		2.46 (97)	2,634	176	6.7	1,973	2,607	1,973	1.335
		3.00 (118)	2,877	379	13.2	2,643	2,607	2,607	1.104
	28.6-mm OSB rated sheathing/Sturd-I-Floor	1.73 (68)	2,290	140	6.1	2,392	4,308	2,392	0.957
		2.46 (97)	3,101	296	9.5	2,460	4,308	2,460	1.261
		3.00 (118)	3,477	518	14.9	3,295	4,308	3,295	1.055
	28.6-mm Structural I PWD	1.73 (68)	2,563	134	5.2	2,392	3,379	2,392	1.072
		2.46 (97)	3,191	235	7.4	2,460	3,379	2,460	1.298
		3.00 (118)	3,738	297	8.0	3,295	3,379	3,295	1.135
Average									1.056
Standard deviation (sample)									0.146
COV (%)									13.8
Minimum									1.335
Maximum									0.750

pull-through strength. F_{brng} in Eq. (6) is based on an assumed 7.62-mm bearing deformation at peak load in connections controlled by a pull-through-type limit state

$$P_{\text{npt}} = (A_{\text{brng}})(F_{\text{brng}}) + 59(G)^{5/2}\pi d \left(\frac{d}{1.414d_1} \right)^2 (t_{\text{WSP}} - 0.762) \quad (6)$$

where F_{brng} = bearing strength at 7.62 mm of bearing deformation (21.9 MPa for OSB and 9.4 MPa for PWD, both rated sheathing and Structural I); A_{brng} = area of bearing under pin head = $\pi/4(d_{\text{hd}}^2 - d^2)$ (mm^2); G = WSP specific gravity; d = pin-shank diameter (mm); d_{hd} = pin-head diameter (mm); d_1 = reference pin diameter = 2.54 mm; and t_{WSP} = nominal thickness of WSP (mm).

For the reported tests, Table 4 compares the measured peak connection strengths (P_{peak}) with the calculated nominal strengths (P_n); the nominal values are based on measured material and geometric properties (Table 2). The average P_{peak}/P_n ratio was 1.056 with an associated 13.8% COV. Although the COV appears high, this value should be viewed in context. For estimating resistance and safety factors, Chapter F of AISI S100 (AISI 2012) recommends a COV of 10% for material properties and 15% for connections different from those explicitly identified in Chapter F. The COV for bearing in wood structural panels is much larger than 15% (APA—The Engineered Wood Association 2013). Thus, in

context, 13.8% is quite good. Fig. 11 compares the measure peak strengths (P_{peak}) and estimated nominal (P_n) connection strengths. The majority of the data points fall within a $\pm 15\%$ band (six data points fall outside the $\pm 15\%$ band, four on the conservative side).

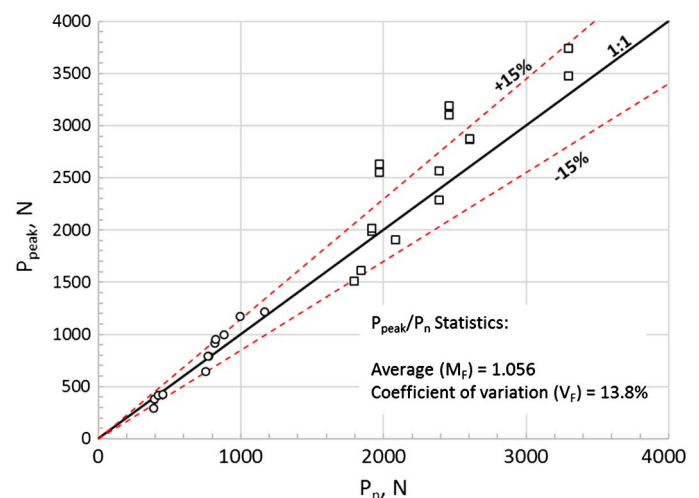


Fig. 11. Peak withdrawal strength from test (P_{peak}) versus calculated nominal strength (P_n)

Table 5. Statistical Parameters/Coefficients

Parameter	Factor		
	Material (<i>M</i>)	Fabrication (<i>F</i>) ^a	Professional (<i>P</i>)
Mean value (<i>M_m</i> , <i>F_m</i> , and <i>P_m</i>)	1.08	1.00	1.06
Coefficient of variation (<i>V_M</i> , <i>V_F</i> , and <i>V_P</i>)	0.10	0.15	0.14
Calibration coefficient (<i>C_φ</i>)	1.52	—	—
Target reliability index (<i>β</i>)	3.50	—	—
Correlation coefficient (<i>C_c</i>)	0.97	—	—
Correction factor (<i>C_p</i>)	1.12	—	—
Coefficient of variation of load effect (<i>V_Q</i>)	0.21	—	—

^aRecommended for connections not listed in AISI S100-12, Chapter F.

By using the statistical analysis procedure provided in AISI S100, Chapter F, Section F1.1(b), resistance and safety factors, ϕ and Ω , respectively, may be determined from Eqs. (7) and (8) for the equilibrium model presented in this paper. Table 5 summarizes the parameters used in Eqs. (7) and (8); the professional factor (P) values are taken from Table 4 data

$$\phi = C_{\phi}(M_m F_m P_m) e^{-\beta_o \sqrt{V_M^2 + V_F^2 + C_p V_P^2 + V_Q^2}} \tag{7}$$

$$\Omega = \frac{1.6}{\phi} \tag{8}$$

By adopting the statistical parameters in Table 5, the withdrawal resistance and safety factors for the withdrawal connections in this paper were determined to be $\phi = 0.573$ and $\Omega = 2.79$.

Thus, it appears that the proposed equations for PO and PT provide a reasonably good estimate of withdrawal strength with the general limits of the WSP and CFS materials tested.

Conclusion

Pneumatically driven hardened steel pins have a long history of use for attaching a variety of substrates to cold-formed steel framing. Pins are often knurled to enhance connection strength at the pin-CFS framing interface. Although knurling configurations may differ between manufacturers, the basic withdrawal response for connections with identical materials (substrate and CFS framing) is essentially the same. In this paper, a general equilibrium model was proposed for the withdrawal strength of connections in which wood structural panels (oriented strand board and plywood) were attached to cold-formed steel. Withdrawal test data from a series of 27 different connection configurations were presented. The tests included seven different wood structural panels, two different pin diameters (from a single manufacturer), and five CFS framing thicknesses. On the basis of test observations, the proposed equilibrium model was calibrated for a particular pin. It was shown that the calibrated model provided an overall reasonable estimate of nominal withdrawal strength with associated resistance and safety factors of 0.573 and 2.79, respectively. To evaluate the general utility of the equilibrium model presented in this paper, additional cross-manufacturer research is suggested.

References

AISI (American Iron and Steel Institute). (2009). "North American standard for cold-formed steel framing—Lateral design." *AISI S213*, Washington, DC.

AISI (American Iron and Steel Institute). (2012). "North American specification for the design of cold-formed steel structural members." *AISI S100*, Washington, DC.

APA—The Engineered Wood Association. (2012). "Panel design specification." *Form No. D510C*, Tacoma, WA.

APA—The Engineered Wood Association. (2013). "Allowable bearing stress for APA wood structural panels." *Technical Topics TT-001B*, Tacoma, WA.

ASTM. (2012). "Standard test method for mechanical fasteners in wood." *ASTM D1761*, West Conshohocken, PA.

ASTM. (2015). "Standard specification for steel sheet, zinc-coated (galvanized) or zinc-iron alloy-coated (galvannealed) by the hot-dip process." *ASTM A653/653M*, West Conshohocken, PA.

ASTM. (2016). "Standard test methods and definitions for mechanical testing of steel products." *ASTM A370*, West Conshohocken, PA.

AWC (American Wood Council). (2014). "National design specification for wood construction." *AWC NDS*, Leesburg, VA.

FPL (Forest Products Laboratory). (2010). "Wood handbook—Wood as an engineering material." *General Technical Rep. FPL-GTR-190*, USDA, Forest Service, Madison, WI.

ICC-ES ESR (International Code Council Evaluation Service). (2014). "Hilti X-GPN MX power-driven fasteners used to attach wood structural panels to cold-formed steel framing." *ICC-ES ESR 3059*, Brea, CA.

ICC-ES ESR (International Code Council Evaluation Service). (2015a). "JAACO Nailpro hardened ballistic pins for attaching gypsum sheathing to cold-formed steel framing." *ICC-ES ESR-2962*, Brea, CA.

ICC-ES ESR (International Code Council Evaluation Service). (2015b). "Power-driven pins for shear wall and diaphragm assemblies with steel framing and wood structural panels." *ICC-ES ESR 2961*, Brea, CA.

ICC-ES ESR (International Code Council Evaluation Service). (2015c). "Stanley bostitch power-driven pins to fasten gypsum board materials to cold-formed steel wall framing." *ICC-ES ESR 3380*, Brea, CA.

ICC-ES ESR (International Code Council Evaluation Service). (2016a). "Gyp-fast fasteners used to attach gypsum sheathing to metal studs." *ICC-ES ESR-2174*, Brea, CA.

ICC-ES ESR (International Code Council Evaluation Service). (2016b). "Ramset plywood fasteners for plywood panel shear walls and diaphragms attached to steel framing." *ICC-ES ER-5380*, Brea, CA.

ICC-ES ESR (International Code Council Evaluation Service). (2016c). "Versapin pneumatic fasteners: Helical-Knurled and Gripshank." *ICC-ES ESR-1641*, Brea, CA.

Morgan, K., Sorhouet, M., and Serrette, R. (2002). "Adhesive applications for shear walls: A pilot study." *Rep. No. CLFSR-12-02*, Dept. of Civil Engineering, Santa Clara Univ., Santa Clara, CA.

Nolan, D. (2009). "Pneumatically driven pins for wood based panel attachments." (<http://www.etf-fastening.com/pdf/CFSEIPinTechNote.pdf>) (Oct. 2009).

Serrette, R., and Nolan, D. (2015). "Pullout strength of steel pins in cold-formed steel framing." *J. Struct. Eng.*, 141(5), 04014144.